Conservation and divergence of meiotic DNA double strand break forming mechanisms in Arabidopsis thaliana

Nathalie Vrielynck, Katja Schneider, Marion Rodriguez, Jason Sims, Aurélie Chambon, Aurélie Hurel, Arnaud de Muyt, Arnaud Ronceret, Ondrej Krsicka, Christine Mézard, et al.

Nucleic Acids Research, 2021 **1**
https://doi.org/10.1093/nar/gkab715

Conservation and divergence of meiotic DNA double strand break forming mechanisms in *Arabidopsis thaliana*

Nathalie Vrielynck[1,†], Katja Schneider[2,†], Marion Rodriguez[1], Jason Sims[2], Aurélie Chambon[1], Aurélie Hurel[1], Arnaud De Muyt[1], Arnaud Ronceret[1], Ondrej Krsicka[2], Christine Mézard[1], Peter Schlögelhofer[2,*] and Mathilde Grelon[1,*]

[1]Institut Jean-Pierre Bourgin, INRAE, AgroParisTech, Université Paris-Saclay, 78000 Versailles, France and [2]Department of Chromosome Biology, Max Perutz Labs, University of Vienna, Vienna Biocenter, Dr. Bohr-Gasse 9, 1030 Vienna, Austria

Received February 01, 2021; Revised July 16, 2021; Editorial Decision August 04, 2021; Accepted August 04, 2021

ABSTRACT

In the current meiotic recombination initiation model, the SPO11 catalytic subunits associate with MTOPVIB to form a Topoisomerase VI-like complex that generates DNA double strand breaks (DSBs). Four additional proteins, PRD1/AtMEI1, PRD2/AtMEI4, PRD3/AtMER2 and the plant specific DFO are required for meiotic DSB formation. Here we show that (i) MTOPVIB and PRD1 provide the link between the catalytic sub-complex and the other DSB proteins, (ii) PRD3/AtMER2, while localized to the axis, does not assemble a canonical pre-DSB complex but establishes a direct link between the DSB-forming and resection machineries, (iii) DFO controls MTOPVIB foci formation and is part of a divergent RMM-like complex including PHS1/AtREC114 and PRD2/AtMEI4 but not PRD3/AtMER2, (iv) PHS1/AtREC114 is absolutely unnecessary for DSB formation despite having a conserved position within the DSB protein network and (v) MTOPVIB and PRD2/AtMEI4 interact directly with chromosome axis proteins to anchor the meiotic DSB machinery to the axis.

INTRODUCTION

During meiosis, maternal and paternal chromosomes recombine and segregate in two consecutive divisions, generating genetically distinct haploid cells. This halving of the genome content is mandatory to prepare for the doubling that occurs during fertilization. In most organisms, correct separation of chromosomes at the first meiotic division relies on the formation of bivalents. These stable structures are connected homologous chromosomes, held together by crossovers (COs) and sister chromatid cohesion. COs, the reciprocal exchange of DNA between two homologous chromosomes, are one of the outcomes of homologous recombination. At least one CO per homologous chromosome pair is required for bivalent formation and subsequent balanced chromosomal segregation (1).

The cascade of events leading to CO formation has been well described (2–4). In most species, formation of the obligatory meiotic COs is ensured at different levels of the meiotic recombination pathway. One is the programmed induction of a large number of CO precursors: the meiotic DNA double strand breaks (DSBs). DSB numbers exceed the final number of COs by several orders of magnitude (5). The cellular toxicity of DNA lesions is well known, suggesting that very robust control mechanisms for meiotic DNA scission and repair must be in place to prevent any meiotic catastrophe. These include the temporal and spatial coupling of meiotic DSB formation with DNA replication, DNA repair, homologous chromosome engagement and synapsis (6–10).

A number of components of the meiotic DSB forming machinery have been identified in several model species. These show variable levels of conservation in terms of protein sequences and/or functions. It is now accepted that the catalytic activity responsible for meiotic DSB formation evolved from an ancestral topoisomerase function still present in *Archaea* and some eukaryotes (Topoisomerase VI) (11). The catalytic part of the Topoisomerase VI-like complex, active during meiosis, is composed of two

*To whom correspondence should be addressed. Tel: +33 1 30833308; Email: mathilde.grelon@inrae.fr
Correspondence may also be addressed to Peter Schlögelhofer. Tel: +43 1 427756240; Email: peter.schloegelhofer@univie.ac.at
†The authors wish it to be known that, in their opinion, the first two authors should be regarded as joint First Authors.
Present addresses:
Arnaud De Muyt, Institut Curie, PSL Research University, CNRS, UMR3244, Paris, France.
Arnaud Ronceret, Instituto de Biotecnología / UNAM, Av. Universidad #2001, Col. Chamilpa C.P. 62210, Cuernavaca, Morelos, Mexico.

subunits of the A monomer, SPO11. They associate to trigger meiotic DSB formation through coordinated transesterification reactions that involve the catalytic tyrosine of each SPO11 monomer together with each DNA strand of the double helix. In *Arabidopsis thaliana* (and probably in plants in general), it is not a homodimer of SPO11 proteins that is active but more likely a heterodimer composed of the two SPO11-1 and SPO11-2 proteins (12–18). In *A. thaliana*, a distant homolog of the archaeal TopoVI B subunit, the MTOPVIB protein, is likely to play a crucial role in SPO11 catalytic dimer formation, since its interaction with each of the SPO11 monomers is required to promote the interaction between SPO11-1 and SPO11-2 (15). The situation could be different in species with homodimeric Spo11 catalytic complexes, as illustrated by the fact that, in *Saccharomyces cerevisiae*, the complex formed between Spo11 and Rec102/Rec104 [related to MTOPVIB, (19)] is monomeric (20). Once DSB formation has been triggered, the SPO11 proteins remain covalently attached to the 5' ends of the broken DNA (21), blocking DSB repair until they are removed by the action of the MRX/N complexes (Mre11 Rad50 Xrs2/NBS1) in conjunction with SAE2/COM1/CtIP (22–27). How DSB formation is coordinated with DSB repair is a largely unanswered question.

Together with the components of the meiotic TopoVI-like complex, additional proteins are essential for meiotic DSB formation (3,5,28). In *S. cerevisiae,* Rec114, Mei4, Mer2, Ski8 and the components of the MRX complex are all required for successful DSB formation. These proteins are all conserved across distant phyla, even if their conservation in terms of primary sequence can be very weak, as is the case for Rec114, Mei4 and Mer2 (29–31). Their role in meiotic DSB formation can also be quite divergent from one species to another. For example, while the MRX complex is strictly required for meiotic DSB repair in all organisms tested, its involvement in meiotic DSB formation is restricted to *S. cerevisiae* and *Caenorhabditis elegans* (28). Similarly, the mRNA decay protein Ski8/Rec103 is required for DSB formation only in fungi (32–34) but probably not outside this kingdom (35). Last, some DSB proteins appear to be completely specific to a given phylum. This is, for example, the case of the recently identified mammalian protein ANKRD31 (36,37) and the *A. thaliana* DFO protein (38). The function of these DSB proteins during meiotic DSB formation is still largely unknown (5,8,28), but they could act as regulators of either the formation or the activation of the catalytic core complex, to trigger DSB formation in a timely and accurately regulated manner.

During meiosis, sister chromatids are structured into chromatin loops emanating from a protein structure called the axis (39). Most of the proteins involved in meiotic recombination, including DSB proteins, are axis-associated whereas DSB sites are located in the loops (40,41). The current working hypothesis proposes that in order to introduce DSBs and promote recombination, some regions of the loops need to be temporarily tethered to the axis (40,41). During these events in *S. cerevisiae*, Mer2 occupies a key position since it establishes a physical link between the chromosome axis and the DSB machinery (42,43). Mer2 is an axis-associated DSB protein, which directly interacts with Mei4 and Rec114 as well as with Spp1, a member of the Set1 COMPASS histone methyl transferase complex responsible for histone methylation at DSB sites. Mer2 in *S. cerevisiae* could therefore be directly involved in the tethering of the DSB sites to the chromosome axis, establishing the indispensable contacts between the DSB catalytic complex located at the loops and the other DSB proteins located at the axis (44).

In this study, we took advantage of the systematic screening for DSB proteins previously performed in *A. thaliana* (45,46) to clarify the cascade of events that occur during the steps of meiotic DSB formation. We methodically investigated the interactions among the DSB proteins and also between the DSB proteins, axis proteins and the DSB processing machinery. We also compared the localization and the epistatic relationships between three of the DSB proteins (MTOPVIB, SPO11-1 and PRD3/AtMER2) during meiosis. Lastly, we revisited the role of PHS1/AtREC114 in order to clarify its involvement in meiotic recombination initiation.

MATERIALS AND METHODS

Plant material and growth conditions

Plants were grown in greenhouses with 70% humidity. *Arabidopsis thaliana* were grown under a 16 h/8 h day/night photoperiod with temperatures of 19 and 16°C for day and night, respectively. *Nicotiana benthamiana* were grown under a 13 h/11 h day/night photoperiod with temperatures of 25 and 17°C for day and night, respectively. The mutant alleles used in the study are listed in Supplementary Table S5.

Construction of vectors for yeast two-hybrid (Y2H) and bimolecular fluorescence complementation (BiFC) experiments

Y2H and BiFC plasmids were constructed as described in (15) by amplifying a full-length or truncated version of the cDNAs with primers flanked by aatB1 and attB2 recombination sites (Supplementary Tables S6 and S7). These were designed to remove the STOP codon from the cDNA. The amplification products were cloned into pDONOR207 (Invitrogen). For Y2H experiments, these entry vectors were used to generate the appropriate expression vectors after LR reactions with pDEST-GADT7 and pDEST-GBKT7 (47) for N-terminal fusions, or pGADCg and pGBKCg (48) for C-terminal fusions. The plasmids pBIFP1 to pBIFP4 (49) were used for BiFC assays. The complete list of pEntry clones generated in this study is given in Supplementary Table S6. Cloning of the full-length cDNAs of *MTOPVIB*, *SPO11-1* and *SPO11-2* was described previously in (15), of *ASY1*, *ASY3* and *ASY4* in (50), of *PRD1* in (51), of *PRD3* in (45), of *NBS1* and *MRE11* in (52). Full-length *SKI8*, *PHS1*, *RAD50* and *COM1* cDNAs were obtained from the *Arabidopsis* stock center (ABRC stock numbers U23481, PENTR221-AT1G10710, U22216 and PENTR221-AT3G52115, respectively). *DFO* and *PRD2* full-length cDNAs were amplified from Col-0 flower buds. The two *DFO* splicing variants described in (38) were amplified using the primers attB1DFO with either attB2DFO.1 or attB2DFO.2. The *PRD2* coding sequence was amplified

using primers MTI20-12#12 and MTI20-12#15 (see Supplementary Table S7 for primer sequences).

Yeast two-hybrid assays

Y2H assays were carried out using the Matchmaker™ GAL4 Two-Hybrid System 3 from Clontech as previously described in (15). Briefly, the yeast plasmids were introduced into AH109 or Y187 strains by lithium acetate transformation. The appropriate pairwise combinations were mated in non-selective media (YPD) and the resulting diploid cells were selected on SD medium lacking the correct combination of amino acids (SD-LW). Interactions were then scored on selective media lacking leucine, tryptophan and histidine (SD-LWH) and adenine (SD-LWHA). All positive interactions were confirmed at least twice. Western blotting was used to verify expression in clones that resulted in negative interactions in all combinations tested as described in (15). The complete set of results is given in Supplementary Table S1.

Bimolecular fluorescence complementation assays

Protein interactions were tested *in planta,* using BiFC assays in *N. benthamiana* leaf epidermal cells expressing a nuclear cyan fluorescent protein (CFP fused to histone 2B) as previously described in (15). Briefly, for each target protein, four expression vectors were produced, generating inactive N- or C- moieties of YFP (YFP^N, YFP^C), fused with the target sequences at either their N- or C-termini. Leaves were infiltrated with *Agrobacterium tumefaciens* cultures transformed with the plasmids for the two candidates to co-express the complementary YFP fusions (Supplementary Table S1, BiFC_detailed results). Results were scored for fluorescence 4 days after infiltration, using a LEICA SP5 II AOBS Tandem HyD confocal laser scanning microscope. The validity of the YFP signal was systematically checked by determining the fluorescence emission spectrum of the signal (Supplementary Figure S1). A negative control was included for each positive interaction detected consisting of each of the fusion proteins of interest expressed together with the complementary YFP moiety fused to unrelated proteins (i.e. DEFICIENS and GLOBOSA) (Supplementary Table S1 and Supplementary Figure S1). All interactions were observed in at least two independent experiments.

Generation of CRISPR-Cas9 *phs1* mutants

Single guide RNAs targeting the *AtPHS1* gene (At1g10710) were chosen using the CRISPOR selection tool (http://tefor.net/crispor/crispor.cgi) (53). The target locus was selected in the first *PHS1* exon (sgRNA-PHS1#1: aaaccgccgtagaaacgc) (Supplementary Figure S6). Details of the experiments for generating *phs1-2* and *phs1-3* alleles are given in Supplementary Materials and Methods.

Transgenic plant lines expressing AtSPO11-1-cMYC

An AtSPO11-1 expression construct was generated to express an 18x cMYC tagged genomic clone of *AtSPO11-1* under the control of its native promoter (see Supplementary Materials and Methods for details). The construct was introduced into a *spo11-1-2* mutant background. Plant lines that were homozygous for both the *AtSPO11-1-cMYC* transgene and the *spo11-1-2* mutation were used for further investigation.

Cytology

Seeds were counted after siliques clearing in 70% ethanol. Meiotic chromosome spreads were DAPI-stained as described in (54). Immunostaining was carried out either on spread male meiotic cells as described in (55) and (56) or on 3D-preserved male meiocytes as described in (57). The primary antibodies used were as follow: guinea pig α-ASY1 (1:250) (57), chicken α-ASY1 (1:50) (this study), guinea pig α-ASY1 (1:10 000) (58), rabbit α-DMC1 (1:20) (59), rat α-ZYP1 (1:250) (60), rabbit α-MLH1 (1:200) (56), rabbit α-MTOPVIB (1:750; 1:400 for super-resolution experiments) (15), rat α-REC8 (1:250) (61), rat α-RAD51 (1:100) (62), rabbit α-SCC3 (1:500) (63), rabbit α-ASY3 (1:300) (64), α-cMYC (abcam ab9106) (1:500), rat α-PRD3 (1:20) (this study) and rabbit α-HEI10 (1:250) (65). Rat α-PRD3 and chicken α-ASY1 antibodies productions are described in Supplementary Materials and Methods. MTOPVIB, HEI10, DMC1 and RAD51 immunofluorescence studies were performed on 2D lipsol spread meiocytes as described in (55) together with either α-REC8 or α-ASY1 as axis staining markers or α-ZYP1 as a synapsis marker. Images were taken using a Zeiss Axio Observer microscope. MTOPVIB, DMC1 and RAD51 foci number were quantified in Fiji, using a semi-automatized procedure as described in (66). MLH1 immunofluorescence studies were carried out on 3D preserved meiocytes as described in (57). Images were acquired using a Leica confocal microscope TCS SP8 AOBS (Acousto-Optical Beam Splitter) (Leica Microsystems) with a 100× HCX PL APO, 1.4 NA immersion objective. Fluorescent signals were recorded using the Lightning mode of LASX software. *Z*-stacks with 0.13 μm intervals were acquired and deconvolved using Lightning default parameters and the adaptative-vectashield option. MLH1 foci were counted using Imaris Spot tool. Slides for PRD3 and SPO11-1-cMYC immunofluorescence and for PRD3 or MTOPVIB STED nanoscopy were prepared as described in (58,62,67). Before mounting the slides with ProLong Glass medium (Invitrogen) they were washed twice in 2× SSC. The secondary antibodies were anti-rat STARRED 1:100 (only for STED Abberior), anti-rabbit Alexa 568 1:400 (Abcam, also used for STED), anti-rat Alexa 568 (ThermoFisher) and anti-guinea pig Alexa 488 (ThermoFisher). Immunostained nuclei detecting PRD3 or SPO11-1-cMYC were imaged with a conventional fluorescence microscope (Zeiss Axioplan2) and appropriate filters. *Z*-stacks with 100 nm intervals were acquired, deconvolved using AutoQuantX software and are presented as projections made with HeliconFocus software. Super-resolution images (PRD3 or MTOPVIB) were acquired using the Abberior STEDYCON system. Protein foci were counted manually with the help of the count tool in Adobe Photoshop. The distance of foci from the axis was measured with Adobe Photoshop.

Scatter dot plots and statistical analyses were performed using the GraphPad Prism 6 software. Statistical

methods used were either two-sided Student's *t* test or one-way ANOVA with multiple comparison procedure. A significance level of $\alpha = 0.01$ was chosen for all analyses.

RESULTS

The *A. thaliana* DSB protein network and its association with the chromatin axis and DNA repair machinery

In order to gain insights into the function of the proteins involved in meiotic DSB formation, we systematically tested the interactions among them as well as with the axial element proteins ASY1, ASY3 and ASY4. We used a combination of yeast two-hybrid (Y2H) and bimolecular fluorescence complementation assays (BiFC or Split-yellow fluorescent [YFP]) as described in (15). We also included Rec114 (PHS1) and Ski8 homologs (35,68) in the Y2H assays. A summary of the results is shown in Figure 1 with the complete set of data in Supplementary Table S1.

Overall, this interaction study revealed several important features. First, the catalytic components of the meiotic DSB machinery (SPO11-1 and SPO11-2) show few direct interactions with the DSB proteins other than MTOPVIB and no direct interactions could be detected with the axial proteins ASY1/3/4. In contrast to the situation in *S. cerevisiae*, no interaction could be detected between AtSKI8 and SPO11 proteins (Supplementary Table S1), consistent with previous reports suggesting that in *A. thaliana* SKI8 is not involved in meiotic recombination (35).

Second, we found that the MTOPVIB protein plays a central role in the meiotic DSB protein network. We previously showed that the MTOPVIB interaction with SPO11-1 and SPO11-2 is necessary to promote the interaction between the two SPO11 paralogs (15). MTOPVIB has also been shown to interact with PRD1 (69). Here we found that in Y2H assays, MTOPVIB establishes a direct interaction with most of the DSB proteins, with the notable exception of PRD3/AtMER2. Hence, it is likely that MTOPVIB establishes a connection between the catalytic components of the complex and its regulatory factors. We previously showed that the last 149 amino acids of MTOPVIB (MTOPVIB$^{345\text{-}493}$) were sufficient to establish the interaction with the N- terminal regions of SPO11-1 and SPO11-2 (15). We refined this finding by showing that the divergent C-terminal domain of MTOPVIB (aa 435 to 493) is dispensable for these interactions (Figure 1D and Supplementary Table S1), restricting the interaction domain to 90 aa (MTOPVIB$^{345\text{-}434}$) that correspond to the MTOPVIB b4 conserved motif defined in (15). This restricted interaction interface is specific to the interactions with the SPO11 proteins. The interactions with the other DSB proteins involve much larger domains of MTOPVIB (Figure 1D and Supplementary Table S1).

Third, our results combined with those of Tang *et al.* (69) reveal that the PRD1 protein also occupies a central position within the meiotic DSB protein network. PRD1 interacts with all the DSB proteins, suggesting that it could act as a platform, possibly supporting the confluence among DSB proteins. Its direct interaction with AtMER2/PRD3 shows that one important function of PRD1 is to connect AtMER2 to the other components of the DSB forming machinery. Truncation of PRD1 to various subdomains revealed that the N-terminal domain of PRD1 is crucial for most of the interactions (all but with AtMEI4/PRD2). In the case of AtMEI4/PRD2, both the N- and C-terminal domains of PRD1 are involved (Figure 1D and Supplementary Table S1).

In *S. cerevisiae* and mouse, Rec114, Mei4 and Mer2 (IHO1 in *Mus musculus*) are proposed to form a functional entity [the RMM (Rec114-Mei4-Mer2) complex] based on various evidence including a direct interaction among them (see Discussion). Our study of the *A. thaliana* homologs revealed a direct interaction in Y2H between AtREC114 (PHS1) and AtMEI4 (PRD2). However, no direct interaction was detected between AtMER2 (PRD3) and the other two RMM-like components. Instead, our Y2H assay revealed strong interactions between the plant-specific DFO, AtREC114 (PHS1) and AtMEI4 (PRD2) proteins. Overall, in the DSB interaction network we found that AtMER2 (PRD3) establishes very few direct interactions with any of the DSB proteins except with PRD1. A previous study (52) reported that PRD3 interacts with MRE11 protein in *A. thaliana*. We therefore tested for possible interactions between AtMER2 (PRD3) and components of the resection machinery: MRE11, RAD50, NBS1 and COM1. We confirmed the interaction between PRD3 and MRE11 and also detected an interaction with COM1 (Figure 1C and Supplementary Table S1), showing that, in *Arabidopsis*, AtMER2 (PRD3) establishes a link between the DSB-forming and resection machineries. MRE11 immunostaining was similar in wild-type and *prd3-3* backgrounds (Supplementary Figure S2) suggesting that interaction of PRD3 with the resection machinery *per se* is not necessary for MRE11 loading and/or stability.

Finally, we explored the possible links between the DSB forming proteins and the axis. We focused on the ASY proteins (ASY1, ASY3 and ASY4), the functional homologs of the mammalian HORMADs/SYCP2/SYCP3 respectively (Hop1/Red1 in *S. cerevisiae*). We and others have shown previously that ASY1 interacts with ASY3 and that ASY3 interacts with ASY4 (50,64,70,71). Here we found that among the DSB proteins, MTOPVIB and PRD2/AtMEI4 establish robust interactions with the three axis components ASY1, ASY3 and ASY4. In contrast, PHS1, DFO, PRD1 and PRD3, interacted with only some but not all of the tested axis components (Figure 1 and Supplementary Table S1).

Formation of SPO11-1-cMYC foci on meiotic chromatin depends on catalytic core complex partners

In order to study SPO11-1 dynamics during *Arabidopsis* meiosis we tagged the C-terminus of SPO11-1 with 18 cMYC epitopes and complemented the *spo11-1-2* mutant (Supplementary Figure S3). We then analyzed the spatial and temporal localization of SPO11-1-cMYC during male meiosis using a specific antibody against the cMYC epitope. We observed that SPO11-1-cMYC forms numerous foci on chromosomes from early leptotene (defined as nuclei with a materializing chromosome axis characterized by a discontinuous ASY1 signal), zygotene and throughout pachytene (Figure 2A) (161 foci ± 30 [$n = 13$] in leptotene nuclei; 173 foci ± 46 [$n = 12$] in zygotene nuclei; 239 foci ± 30 [$n = 9$]

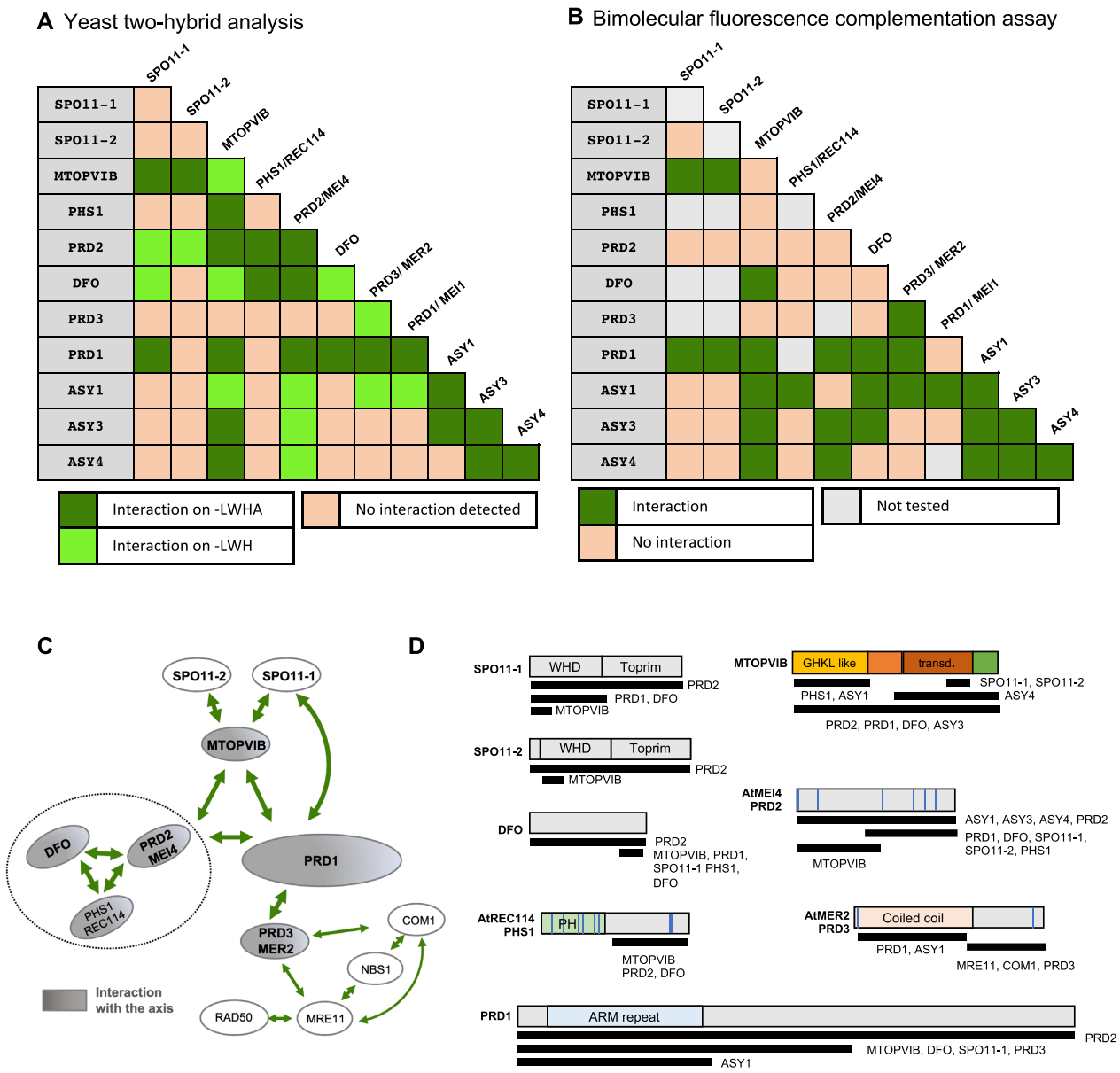

Figure 1. The DSB protein interaction network. (**A**) Summary of the yeast two-hybrid assay results. Dark green indicates growth on SD-LWHA for at least one of the combinations tested (involving either full-length or truncated versions of the tested proteins). Light green indicates growth on SD-LWH medium for at least one of the combinations tested. Pink indicates that none of the combinations tested conferred auxotrophy. The complete set of results is given in Supplementary Table S1. (**B**) Summary of the bimolecular fluorescence complementation (BiFC) assays. Green indicates that an interaction was detected with at least one of the combinations tested. Pink indicates that none of the combinations tested conferred a YFP signal. Gray indicates that the interaction was not tested. The complete set of results is given in Supplementary Table S1. Interactions of PRD1 with SPO11-1, SPO11-2, MTOPVIB, PRD3 and DFO correspond to results reported by (69). (**C**) Schematic representation of the interaction network. Green arrows: Strong interactions between two proteins. Bold letters: proteins essential for DSB formation. Gray shapes: Proteins that directly interact with axial proteins ASY1, ASY3 or ASY4. (**D**) Detailed depiction of interaction domains defined in yeast two-hybrid assays. Schematic representation of the DSB proteins with their functional domains (WHD for winged-helix domain, transd. for transducer domain, PH for pleckstrin homology domain). Blue vertical bars indicate structurally conserved motifs. Below each protein, black bars represent the regions that interact with the proteins indicated on the right or below the bars.

in pachytene nuclei; Figure 2 and Supplementary Table S2). These data are consistent with results published in (72).

SPO11-1-cMYC was detected on spreads of meiotic chromatin in *prd1*, *prd2*, *prd3*, *dfo*, *spo11-2* and *mtopVIb* mutant lines (Figure 2, Supplementary Figure S4 and Supplementary Table S2). All these mutants are synapsis-defective therefore we could only discriminate early leptotene stages (when the ASY1 signal is not yet linear) from the rest of prophase (when the ASY1 signal is linear). In meiocytes of *prd1, prd3* or *dfo*, SPO11-1-cMYC foci numbers were not significantly different to those in wild-type throughout prophase (Figure 2). While wild type-like SPO11-1-cMYC plants had on average 186 foci (± 48, $n = 34$; all prophase stages), *prd1* mutants had 156 (± 33, $n = 26$), *prd3*

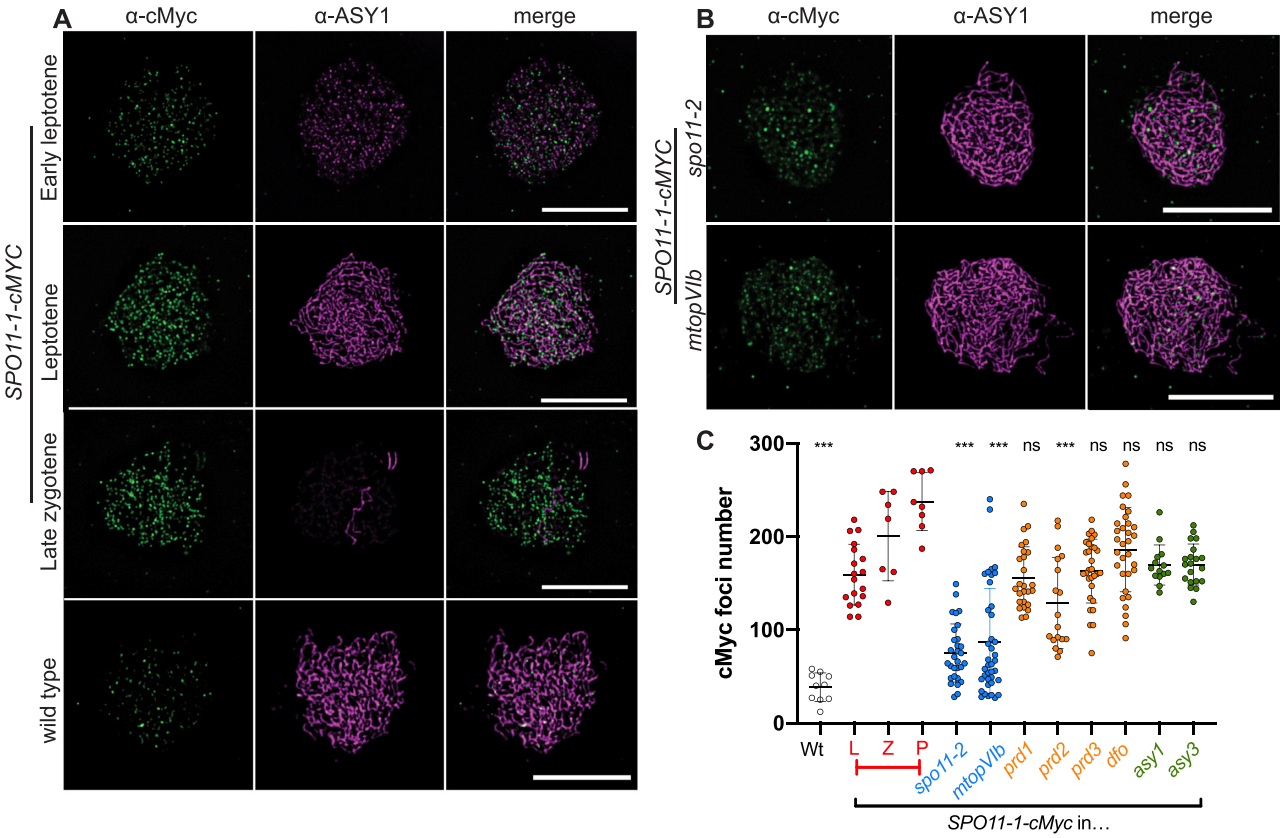

Figure 2. Immunolocalization of SPO11-1-cMYC on spreads of male meiocytes. (**A**) Co-immunolocalization of the axis protein ASY1 (magenta) and SPO11-1-cMYC (green) in SPO11-1-cMYC expressing plant lines (containing the *spo11-1-2*$^{-/-}$ mutation) and wild-type (Col-0) (without *SPO11-1-cMYC*); size bar: 10 μm. (**B**) Detection of SPO11-1-cMYC foci in *spo11-2-3* and *mtopVIb* mutants; size bar: 10 μm. (**C**) Quantification of SPO11-1-cMYC foci in Col-0 (Wt), *spo11-1-2* (L: leptotene, Z: zygotene, P: pachytene), *spo11-2-3*, *mtopVIb-2*, *prd1-2*, *prd2-1*, *prd3-4*, *dfo-2, asy1-2* and *asy3-1* (see Supplementary Figure S4). Statistical analysis was used to compare the mean of SPO11-1-cMyc in *spo11-1-2* (all stages included) to the mean of all other plant lines indicated (one-way ANOVA, with Dunnett correction for multiple comparisons, 99% confidence interval; ns, $0.01 < P$; *** $P < 0.0001$; error bars represent SD).

mutants 163 (±34, $n = 30$) and *dfo* mutants 186 (±45, $n = 32$) foci (combined prophase stages). The *prd2* mutant, however, showed a slight but significant reduction in foci numbers with an average of 129 (±49, $n = 18$) foci.

Remarkably, mutants related to factors of the DSB forming core complex, SPO11-2 and MTOPVIB, had significantly lower SPO11-1-cMYC foci numbers when compared to the wild type-like SPO11-1-cMYC plants (75 ± 31, $n = 30$ and 87 ± 58, $n = 39$ in *spo11-2* and *mtopVIb*, respectively). These findings suggest that normal association of SPO11-1-cMYC with meiotic chromatin requires the presence of SPO11-2, MTOPVIB and to some extent PRD2 but not of PRD1, PRD3 or DFO.

MTOPVIB foci formation is independent of most of the DSB proteins with the exception of DFO and SPO11-1

MTOPVIB forms foci associated with meiotic chromosomes from leptotene to pachytene. These foci are abolished in *spo11-1* but not in *spo11-2* mutant backgrounds (15). Here, we investigated MTOPVIB dynamics during male meiosis in more DSB-defective backgrounds. In wild-type, the number of MTOPVIB foci is on average 192 ± 53 (mean ± SD, $n = 97$). In *prd1*, *prd2* and *prd3* mutants, no significant differences in MTOPVIB foci numbers were observed (Figure 3 and Supplementary Table S3). Mutation of *DFO* does, however, modify MTOPVIB abundance. An almost two-fold increase (353 ± 134, n = 32) in the number of foci was observed in *dfo-1* mutants (Figure 3 and Supplementary Table S3). These results reveal that among all the DSB proteins, DFO is a negative regulator of MTOPVIB loading and/or stabilization onto chromatin.

Foci formation of the core complex proteins SPO11-1-cMYC and MTOPVIB is largely independent of the axial proteins

We then investigated whether SPO11-1-cMYC and MTOPVIB foci formation is dependent on the presence of a fully intact axis. As shown in Figure 2 and Supplementary Figure S4, no changes to SPO11-1-cMYC foci numbers were detected in either *asy1* or *asy3* (170 ± 21.5 and 170 ± 22, respectively). MTOPVIB foci were only slightly modified by mutations affecting the axial elements (Figure 3 and Supplementary Table S3). In wild-type, 192 ± 53 ($n = 97$) MTOPVIB foci can be detected (all prophase stages included). In the *pch2* and *asy1* mutants,

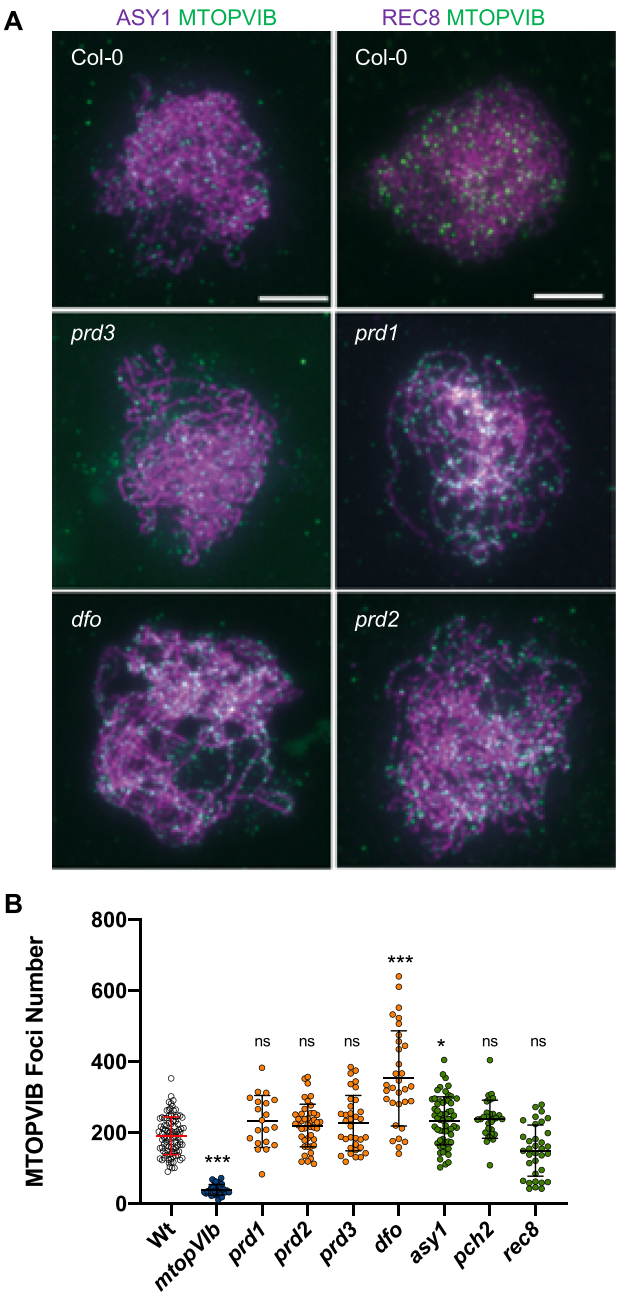

Figure 3. Immunolocalization of MTOPVIB on spreads of male meiocytes. (**A**) Co-immunolocalization of an axis protein (ASY1 or REC8, magenta) together with MTOPVIB (green); scale bar: 5 μm. (**B**) MTOPVIB foci counts in various mutant backgrounds. Statistical analysis compares mean foci numbers in each mutant to wild-type mean (one-way ANOVA with Dunnett correction for multiple comparison, 99% confidence interval; ns, $0.01 < P$; * $0.001 < P < 0.01$; *** $P < 0.0001$; error bars represent SD). Alleles investigated were *mtopVIb-2*, *prd1-2*, *prd2-1, prd3-3*, *dfo-1, asy1-4*, *pch2-1* and *rec8-3*.

the numbers increased moderately (238 ± 54, $n = 30$ and 233 ± 68, $n = 60$, respectively), whereas in the *rec8* mutant they decreased slightly (150 ± 72, $n = 34$). These findings show that an intact axis is not crucial for loading the DSB catalytic machinery core to chromatin but can affect its abundance or stability.

PRD3/AtMER2 forms axis associated foci that depend on ASY1 and ASY3

To analyze the dynamics of PRD3/AtMER2 during male meiosis, we raised an antibody against its N-terminus (AA 1–125). We observed that PRD3/AtMER2 appears early during prophase, before the axis signal is linear and forms numerous foci on unsynapsed chromosome axes during leptotene and zygotene (171 ± 48, $n = 28$; Figure 4 and Supplementary Figure S5). This number strongly decreases as synapsis proceeds to an average level of 40 foci (±22, $n = 12$) at pachytene. To analyze the localization of PRD3 relative to the meiotic axis, we obtained images using STED nanoscopy. In leptotene, PRD3 localizes pre-dominantly with foci or stretches of the meiotic chromosome axis proteins ASY1 (Supplementary Figure S5) or ASY3 (Figure 4A). During zygotene and pachytene, PRD3 foci can still be detected, but mostly detected co-localizing with the unsynapsed parts of the chromosome axis (Figure 4A). The distance of PRD3 foci to the axis was measured on four leptotene, five zygotene and two pachytene cells. This showed a close association of PRD3 foci with axes of unsynapsed chromosomes (56 nm ± 22, $n = 80$) and a distant association with axes after synapsis (144 nm ± 72, $n = 46$; Figure 4A).

Having established that PRD3 colocalizes with the meiotic axis, we were interested in whether PRD3 localization depends on meiotic axis proteins. In both *asy1* and *asy3* mutant nuclei, PRD3 foci numbers drop strongly from 171 ± 48 ($n = 28$) in wild-type to 65 ± 33 ($n = 31$) and 39 ± 24 ($n = 28$) foci/cell respectively (Figure 4C, Supplementary Figure S5 and Supplementary Table S4), suggesting that PRD3 foci formation/stabilization on the axes is largely dependent upon these two proteins.

To test whether PRD3 binding to meiotic chromatin depends on further DSB promoting proteins, we analyzed its localization and abundance in meiocytes of mutants depleted of different members of the DSB forming complex (Figure 4C, Supplementary Figure S5 and Supplementary Table S4). In all mutant lines PRD3 foci numbers were significantly reduced compared to wild-type (P value < 0.0001; ANOVA). While 171 (±48, $n = 28$) foci were counted in wild-type leptotene cells, only 96 (±38, $n = 21$), 85 (±34, $n = 21$) and 95 (±29, $n = 30$) were detected in *prd1, prd2* and *dfo*, respectively. Even less foci were observed in mutants lacking a member of the catalytic core subunit (*spo11-1,* 51 ± 34, $n = 33$; *spo11-2,* 66 ± 35, $n = 34$*; mtopVIb,* 77 ± 30, $n = 15$ and *spo11-1 spo11-2* 70 ± 37, $n = 39$).

We also analyzed MTOPVIB localization relative to the axis by STED nanoscopy. We observed that as prophase progresses and synapsis takes place, MTOPVIB foci are located further away from the axes, with an average distance of 70 nm (±31, $n = 75$) at unsynapsed axes to 104 nm (±46, $n = 80$) at synapsed axes (Figure 4B). Lastly, we performed a colocalization study on MTOPVIB and PRD3 in male meiocytes. We observed that the windows of expression of PRD3 and MTOPVIB are not completely similar, with PRD3 appearing and disappearing earlier than

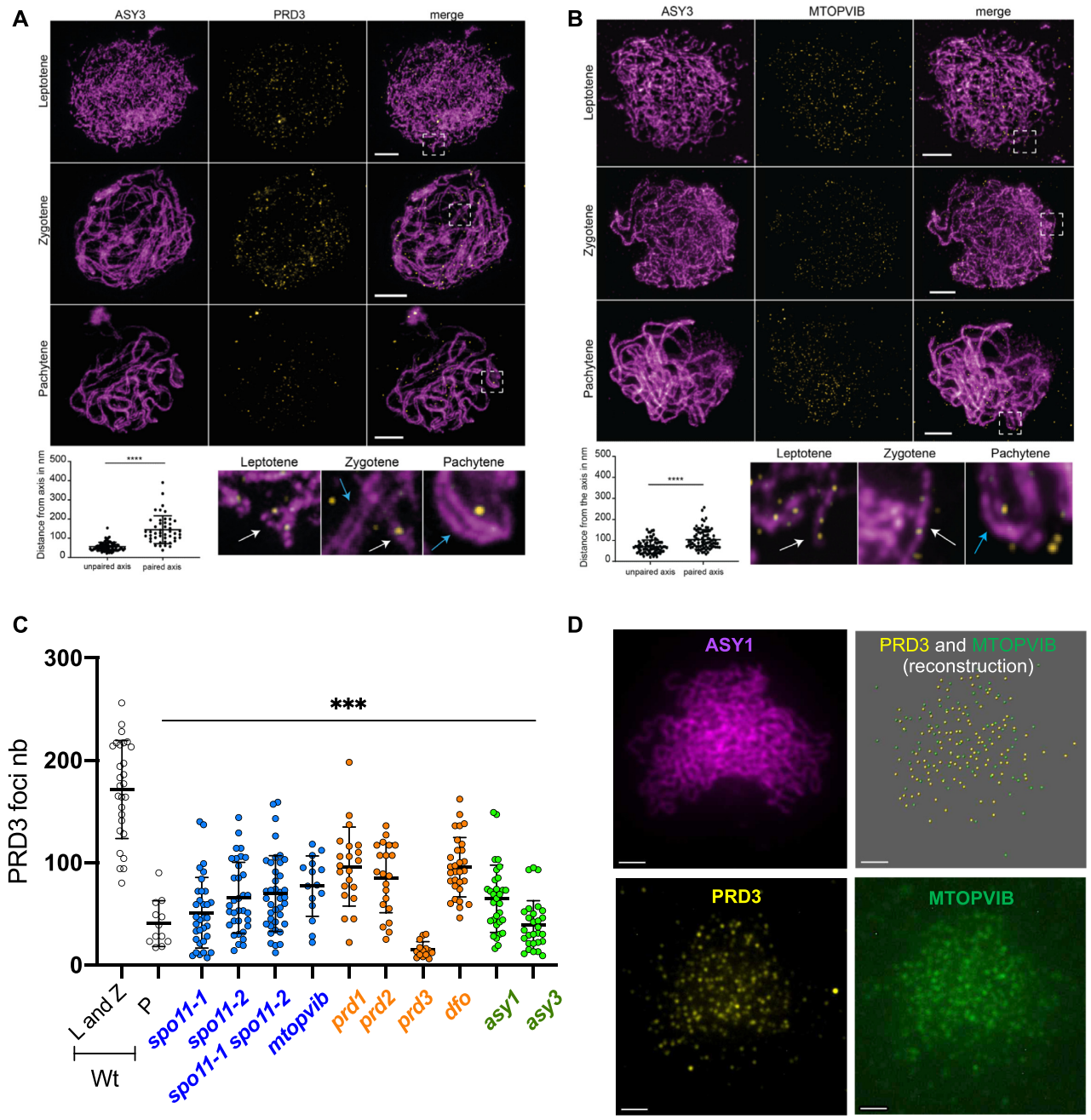

Figure 4. AtMER2/PRD3 and MTOPVIB form non-overlapping foci, more tightly associated with unpaired axes than paired axes. (**A** and **B**) Co-immunolocalization of the axis protein ASY3 (magenta) with either PRD3 (A, yellow) or MTOPVIB (B, yellow) using STED nanoscopy. Enlargements correspond to the boxes indicated with dashed white lines. White arrows indicate unpaired axes, and blue arrows indicate paired axes. Graphs represent the distances measured from foci to the unpaired or paired meiotic axes. Differences between the mean values were evaluated (non-parametric Mann–Whitney test; **** $P < 0.0001$; error bars represent SD); size bar: 2 μm. (**C**) Quantification of PRD3 foci in Col-0 (Wt, L: leptotene, Z: zygotene, P: pachytene), *spo11-1-2, spo11-2-3*, *spo11-1-2 spo11-2-3, mtopVIb-2*, *prd1-2*, *prd2-1*, *prd3-4*, *dfo-2, asy1-2* and *asy3-1* plants (see Supplementary Figure S5). Statistical analysis was used to compare the mean of Col-0 (leptotene/zygotene) to the mean of each mutant (one-way ANOVA, with Dunnett correction for multiple comparison, 99% confidence interval; ns, $0.01 < P$; *** $P < 0.0001$; error bars represent SD). (**D**) Co-immunolocalization of the axis associated protein ASY1 (magenta), PRD3 (yellow) and MTOPVIB (green). The reconstructed image shows the detected PRD3 (yellow spheres) and MTOPVIB foci (green spheres) using the Imaris spot detection tool. Hardly any colocalization could be detected; size bar: 5 μm.

MTOPVIB. At leptotene, when large numbers of foci related to both proteins are visible on chromosomes, hardly any colocalization could be detected between them (Figure 4D).

Is AtREC114/PHS1 involved in meiotic recombination initiation?

Interaction studies revealed that AtREC114/PHS1 interacts with several components of the meiotic DSB machinery (see above). We therefore examined its role in meiotic DSB formation. Previously, *Atphs1* mutants were reported (68) to be required for RAD50 import into the nucleus. We therefore investigated the phenotype of *phs1-1* mutants described in (68) as well as additional publicly available insertion lines (Figure 5A). Under our experimental conditions, none of these insertion alleles displayed phenotypes related to fertility or chiasma formation (Supplementary Figure S6), raising the possibility that either these alleles are leaky or that the AtREC114/PHS1 protein plays no major role in reproduction. In order to clarify this, we generated CRISPR-Cas9 null mutant alleles by targeting the first exon in *PHS1*. We selected two independent lines, hereafter termed *phs1-2* and *phs1-3*, with either a deletion or insertion of a single nucleotide in position 41 of the cDNA (Supplementary Figure S6). These mutations introduce a frameshift at the beginning of the coding sequence of *PHS1* (from codon 14, Supplementary Figure S6). To confirm that the introduced mutations do not modify *PHS1* splicing, we sequenced the *PHS1* cDNA and did not find any differences between wild-type and the mutants. This indicates that both alleles are likely to produce a modified variant of PHS1 of 42 and 91 aa, respectively, sharing only 13 aa with the wild-type PHS1 protein (Supplementary Figure S6). Therefore, it is very likely that *phs1-2* and *phs1-3* mutants are null mutant alleles. Neither of the *phs1-2* and *phs1-3* homozygous mutants showed reduced fertility (seed count) or chiasma formation (Supplementary Figure S6). We then analyzed a number of markers of meiotic progression to decipher whether *PHS1*/*AtREC114* mutation could have an impact on some steps of meiotic recombination. No change in MTOPVIB, RAD51, DMC1 or early HEI10 foci numbers was observed (Figure 5B and C, Supplementary Figure S7). Last, we introduced the *phs1-2* mutation into the DSB-repair-defective mutant *mre11* (73). We observed that the *phs1-2* mutation was unable to suppress any of the fragmentation defects observed in this background (Supplementary Figure S8). Taken together, these data show that meiotic DSB formation and recombination initiation steps are not affected by loss of *PHS1 in Arabidopsis.* Nevertheless, when we quantified class I COs in two *phs1* mutant alleles (*phs1-2* and *phs1-5*), by detecting the MLH1 protein in male meiocytes (Figure 5D), we observed a clear increase in MLH1 foci numbers in both mutants, from 10 ± 1.7 ($n = 73$) foci per cell in wild-type to 11 ± 2 ($n = 243$) in *phs1-2* and 14 ± 2 ($n = 148$) in *phs1-5* mutants. The increase was confirmed using another Class I CO marker (HEI10 staining at late pachytene stage, Supplementary Figure S7). Taken together, these data reveal that REC114 (PHS1) in *Arabidopsis* is clearly not needed for meiotic DSB formation but is nevertheless a regulator of meiotic recombination outcomes.

DISCUSSION

MTOPVIB and PRD1 occupy a central position within the DSB protein network

Systematic investigation of the interactions among the DSB proteins revealed that MTOPVIB and PRD1 directly interact with most of the other DSB proteins (Figure 1). We previously showed that MTOPVIB is a key element of the DSB forming machinery since its interaction with SPO11-1 and SPO11-2 is necessary to promote the interaction between these two SPO11 paralogues (15), which likely promotes the assembly of the core catalytic complex. Here we showed that in addition to this, MTOPVIB is also likely to establish a connection between the catalytic core complex (SPO11-1 and SPO11-2) and most of its regulatory factors. In agreement with this, we observed that SPO11-1-cMYC foci formation is drastically perturbed in the *mtopVIb* mutant, a finding which suggests that MTOPVIB is not only promoting the assembly of the catalytic core complex but also its loading and/or stabilization on chromosomes. We found that PRD3/AtMER2 is the only DSB protein that does not directly interact with MTOPVIB. This recapitulates the situation in *S. cerevisiae*, where the Rec102/Rec104 dimer [which is distantly related to the MTOPVIB/TopoVIBL protein family (74)] also interacts with all the other DSB proteins except Mer2 (33). In *A. thaliana*, PRD3/AtMER2 is connected to the other DSB proteins through a direct interaction with PRD1. PRD1 is a large protein of 1330 amino acids showing clear sequence similarities with MmMei1 but without any known homologues outside animals and plants (51,75,76). We found that PRD1 directly interacts with most of the other DSB proteins. This suggests that it could act as a platform to support the association among DSB proteins and therefore likely to promote either the assembly and/or the activation of the meiotic catalytic complex. Its direct interaction with PRD3/AtMER2 shows that one important function of PRD1 is to connect AtMER2 to the other components of the DSB forming machinery, a role that could be conserved in mammals where PRD1 and MER2 homologs (MEI1 and IHO1, respectively) colocalize with the other DSB factors REC114, MEI4 and ANKRD31 (77).

Connection of the meiotic DSB machinery to the axis

An important result of the interaction analyses is that several of the DSB proteins directly interact with one or more of the components of the chromosome axial elements (ASY1, ASY3 and ASY4). Among these, the interactions involving MTOPVIB and PRD2/AtMEI4 were the strongest (Figure 1). This confirms the key position of MTOPVIB in the DSB-forming machinery and suggests that MTOPVIB could play a direct role in connecting the DSB-forming machinery (including the catalytic components SPO11-1 and SPO11-2) to the axis. Further studies are required to decipher whether MTOPVIB's presence is required for the stable axis association of all the other DSB proteins with the axis. However, our finding that the number of PRD3 and SPO11-1-cMYC foci is strongly reduced in the *mtopVIb* mutant background (Figures 2 and 4) is heading in this direction. Despite the direct interaction of MTOPVIB

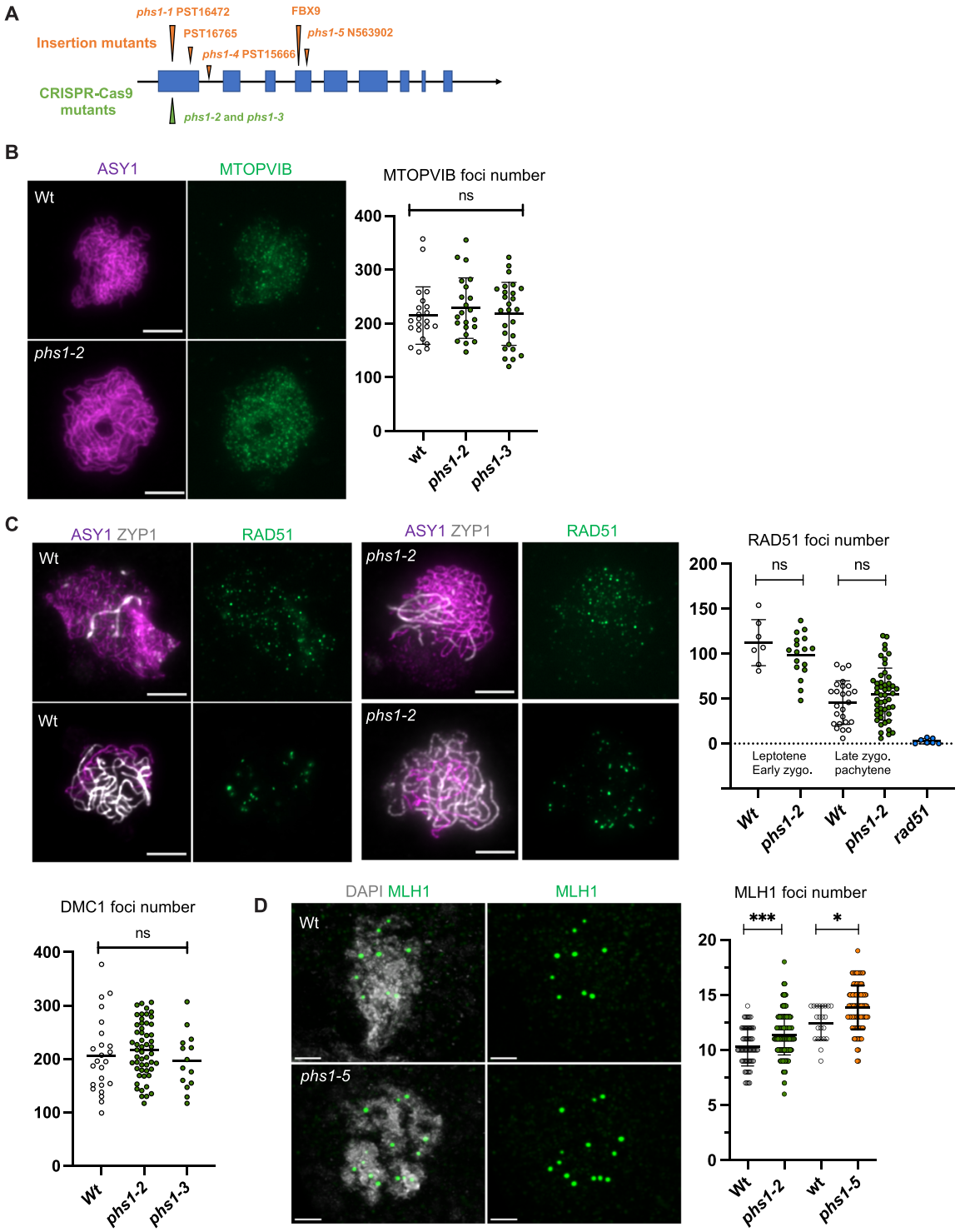

Figure 5. AtREC114/PHS1 is not essential for meiotic DSB formation. (**A**) *AtREC114/PHS1* gene structure. Blue rectangles represent exons. Colored triangles indicate the position of the mutations (insertion lines in orange; CRISPR-Cas9 generated mutants in green). (**B**) Co-immunolocalization of the axis protein ASY1 (magenta) and MTOPVIB (green) in wild-type and p*hs1-2* meiocytes. The graph shows the quantification of MTOPVIB foci numbers. (**C**) Co-immunolocalization of the axis protein ASY1 (magenta), the central element protein ZYP1 (white) and RAD51 (green). Quantification of RAD51 foci according to the level of synapsis is shown. No or low ZYP1 signal, corresponding to leptotene or early zygotene were grouped together; extended ZYP1 signal corresponding to late zygotene and pachytene stages were counted together. Quantification of DMC1 foci in wild-type and mutants is also shown, all stages counted together. (**D**) Immunolocalization of MLH1 in wild-type, p*hs1-2 and phs1-5* meiocytes. The graph shows the quantification of MLH1 foci number on meiocytes at diplotene and diakinesis stages (determined according to ZYP1 staining, not shown); scale bars = 5 μm. Statistical analyses compare mean foci numbers either between wild-type and mutant (MLH1 and RAD51 foci, unpaired Student's *t*-tests) or between all means (MTOPVIB and DMC1 foci numbers, one-way ANOVA, with Tukey correction for multiple comparison). All tests were analyzed using a 99% confidence interval; ns $0.01 < P$; *** $P < 0.0001$; error bars represent SD.

with the axis, we observed that MTOPVIB foci formation is not or only slightly modified in the axis mutants tested, *asy1* and *rec8* (Figure 3), showing that an intact axis is not required for MTOPVIB loading.

So far, the only component of the DSB machinery that has been shown to be involved in the connection to the axis is Mer2 (Rec15 and IHO1 in *Schizosaccharomyces pombe* and mouse, respectively). In *S. cerevisiae* the axial element components Red1 and Hop1 promote axis-localization of Mer2, which in turn recruits Rec114 and Mei4, to assemble the RMM (Rec114, Mei4, Mer2) complex (41,78). In *S. pombe*, Rec15 directly interacts with the axis proteins Rec10 (SpRed1, ASY3) and Hop1 (SpASY1) (79,80) and in mammals IHO1 interacts with HORMAD1 (MmHop1/ASY1) (81). In addition to these direct interactions of Mer2 with several axis components, converging studies revealed that most of the other DSB proteins are dependent upon Mer2 for their association with the chromosome axis, and not vice versa. This is, for example, the case in *Sordaria macrospora* where SPO11::GFP foci are not formed in *mer2Δ* while MER2::GFP foci are formed normally in *spo11Δ* and *ski8Δ* (31). In *S. cerevisiae,* Rec114 and Mei4 foci formation are absolutely dependent upon Mer2 but not the reverse. In mammals, the association of IHO1 with the chromosome axis only depends on axial components and does not change in the absence of MEI4 or REC114. However, as observed in *S. cerevisiae*, MEI4 foci formation is dependent on IHO1 (29,41,81,82). Based on these data, Mer2 was proposed to play a conserved role promoting the assembly of the pre-DSB complex on the chromosome axes, through its dual interaction first with axial components, then with Rec114 and Mei4.

In *A. thaliana* PRD3/AtMER2 interacts with ASY1 in Y2H and BiFC assays (Figure 1 and Supplementary Table S1). Indeed, PRD3/AtMER2 foci numbers are significantly reduced not only in *asy1* (minus 60%) but also in *asy3* (minus 80%) mutants. This is consistent with the fact that regular localization of ASY1 depends on ASY3. It should be noted that DSB formation is only affected in *asy3* but not *asy1* mutants (64,83). This is reminiscent of data in other species such as in *S. pombe* where Hop1 (SpASY1) and Rec10 (SpASY3) act redundantly to recruit Mer2/Rec15 onto the axis (79), with *rec10* mutants showing stronger defects in DSB formation than *hop1* mutants. In contrast to other organisms, PRD3/AtMER2 foci formation is also significantly reduced, but not abolished, in all DSB mutants studied, including *mtopVIb* and *spo11-1* (Figure 4). Conversely, neither MTOPVIB nor SPO11-1-cMYC foci formation are altered in *prd3* mutants (Figures 2 and 4). Therefore, it appears that in *A. thaliana* MER2 is not mandatory for the chromosome localization of the catalytic core DSB proteins (including SPO11-1 and MTOPVIB).

We support a model that predicts independent loading of axis-associated DSB sub-complexes, including PRD3/AtMER2, and loop-associated DSB-core complexes (including SPO11-1 and MTOPVIB). PRD3/AtMER2 could fulfill the evolutionary conserved role of integrating signals from the cell-cycle and the replication machinery to guide the loop-associated DSB sub-complexes to defined sites at the axis. Specific to the model we envisage for plants, PRD3/AtMER2 would only be stabilized at the axis upon interaction of the axis- and loop-localized sub-complexes. The entire DSB complex would be anchored at the axis relying on the various interactions between DSB complex proteins and axis proteins, especially highlighting the central role of MTOPVIB. In line with our observations, we propose that in the absence of the other DSB factors, PRD3/AtMER2's residence time at the meiotic axis would be very limited. MTOPVIB and SPO11-1-cMYC (and most likely also SPO11-2) are highly abundant on meiotic chromatin and only a sub-fraction of these proteins will be involved in generating meiotic DSBs. The hyper-abundance of the core-complex components and their long-lasting chromatin association [until pachytene, Figure 2 and (15)] suggests that the DSB core sub-complex is inactive until it encounters all other partners of the DSB complex. This would include the axis-associated PRD3, apparently needed to activate the transesterification reaction.

Minimal conservation of the RMM complex in *A. thaliana*

Rec114, Mei4 and Mer2 were first shown to form a stable complex in *S. cerevisiae* (33,84) and this was then confirmed in *S. pombe* (80). In mouse, the three proteins may also form a functional entity since direct interactions were found between Mei4 and Rec114 (29). Our study revealed a direct interaction between AtREC114 (PHS1) and AtMEI4 (PRD2) but none was detected between AtMER2 (PRD3) and any of the other RMM-like components. Instead, we revealed a strong interaction in yeast two-hybrid assays between the three proteins DFO, AtREC114 (PHS1) and AtMEI4 (PRD2), suggesting that DFO but not MER2 tightly associates with AtMEI4 and AtREC114 to regulate DSB formation. DFO is a small protein of <300 aa for which no homologs outside the plant kingdom have been identified (38). Interestingly, two splicing variants of the *DFO* gene were identified (38). The two variants differ at their 3' ends: *DFO.1* is predicted to generate a protein of 233 aa while *DFO.2* is 44 aa longer (Supplementary Table S1 and (38)). We found that the large majority of the interactions detected with the DFO protein were specific to the longer variant, DFO.2 (except for PRD2, Figure 1D, Supplementary Table S1). This allows us to restrict the interaction domain of DFO with the other DSB proteins (except PRD2) to the last 44 aa and suggests that alternative splicing of *DFO* described in (38) represents a regulatory mechanism for DFO function. The existence of splicing variants has been extensively reported, including for meiotic genes (17,85), but the functional relevance of this splicing is unknown in the large majority of the cases. One notable exception is the situation of the mammalian *SPO11* gene for which two versions, α and β are transcribed. The β-form appears to be the only one which functions in meiotic DSB formation in autosomes (86) because of its capacity to interact with TopVIBL, the mammalian homolog of MTOPVIB (74). We observed that DFO is expressed as two variants, but only one establishes a direct interaction with AtREC114, PRD1, MTOPVIB and SPO11-1. This suggests that a similar mechanism of transcriptional splicing regulation might be involved and play a role either in the assembly and/or the stabilization of the *Arabidopsis* complex formed

by DFO with AtREC114/PHS1 and AtMEI4/PRD2. Interestingly, MTOPVIB foci numbers are significantly higher in *dfo* mutants, suggesting it plays an important role in regulating the abundance of a key component of the meiotic DSB complex.

The involvement of the *Arabidopsis* REC114/PHS1 in a divergent RMM-like complex raised the question of its precise role in meiotic DSB formation. While the Rec114 protein sequence is poorly conserved (30,31) in all species investigated so far, Rec114 plays a key role in meiotic DSB formation (29,87–91). In contrast, we found that *Arabidopsis phs1* mutants are completely fertile and show no obvious alteration of meiotic DSB formation with normal DMC1, RAD51, and early HEI10 foci formation and dynamics (Figure 5 and Supplementary Figure S7). It has to be noted that we cannot exclude the possibility that none of the *phs1* allele investigated is null. But this appears very unlikely considering that we have analyzed seven independent lines, corresponding to mutations covering the whole coding sequence. In maize however, the *phs1* mutant is completely sterile, a phenotype associated with an absence of RAD51 foci formation and occurrence of non-homologous synapsis (92). These phenotypes are also observed in the maize *spo11-1* mutant (17), therefore we propose that, in maize, REC114 function is conserved and that PHS1 is required for meiotic DSB formation. Such discrepancies in the function of conserved meiotic genes have already been described, notably concerning the mechanisms of meiotic DSB formation. For example, the two genes $P31^{COMET}$ and *PCH2* are essential for meiotic DSB formation in rice (93,94) but not in *A. thaliana* (95–97). Rice together with maize and *Arabidopsis* belong to two distinct classes of flowering plants (monocotyledons and dicotyledons) that diverged approximately 150 Mya ago (98). Our results suggest that the requirement for REC114 in DSB formation could have been lost in the dicotyledon lineage (*Arabidopsis*) but not in the monocotyledons (rice and maize). Nevertheless, we also demonstrate in this study that AtREC114 has retained its place among the DSB protein network, suggesting that even if *Arabidopsis* REC114/PHS1 is unnecessary for meiotic DSB formation, it likely participates in regulating some aspect of meiotic recombination. Our finding that MLH1 and late HEI10 foci numbers are increased in the absence of PHS1 supports this idea (Figure 5 and Supplementary Figure S7). A finding also in agreement with the recent discovery that, In *S. cerevisiae*, the RMM proteins form clusters on which the other DSB proteins as well as additional regulatory proteins could be recruited, promoting not only the assembly and the activation of the DSB core complex but, possibly, also regulating further steps of DSB repair (99).

A possible role of AtMER2/PRD3 in coordinating meiotic DSB formation with subsequent repair

In all organisms studied so far, Mer2 is a central component of the meiotic DSB machinery. It mediates the formation of the pre-DSB complexes by establishing a link between the axis and the DSB machinery at least in yeasts, mouse and *Sordaria*. As discussed above, our data suggest that MER2/PRD3 proficiency in assembling in a canonical RMM complex is not conserved in *A. thaliana*. However, our study revealed that PRD3 interacts with the two DNA processing and repair proteins MRE11 and COM1. These proteins are part of the meiotic DSB repair machinery (MRN complex-MRE11, RAD50, NBS1 and COM1-also known as SAE2/CtIP) and are both required for DSB processing, SPO11-oligo generation and correct DSB resection. While the *prd3* mutant is defective in DSB formation, *mre11* and *com1* are defective in DSB repair. Meiosis in *mre11* and *com1* mutants is characterized by strong chromosome fragmentation at the metaphase I/anaphase I transition (25,73). Direct interaction between PRD3 and these two components of the DSB resection machinery suggests that PRD3 has a role in either recruiting or activating the DSB resection machinery, thereby allowing coordination between DSB formation and DSB repair. In *S. cerevisiae,* there is also a connection between Mer2 and the MRX complex since ScMer2 interacts in a yeast two-hybrid assay with Xrs2 (ScNBS1) and MRE11 (33). However, since the MRX complex is required for the DSB formation step itself in *S. cerevisiae*, a possible role in coordinating DSB formation and DSB repair has not been investigated. This potential role of AtMER2/PRD3 in coordinating DSB formation and the initial resection steps of homologous recombination can be put in parallel with the recent findings obtained in *S. macrospora*: Mer2 is needed for pre-DSB complex assembly and also for subsequent meiotic recombination, since it is required to promote spatial pairing and synapsis of the homologous chromosomes (31). It would be interesting to test whether these post-DSB functions of Mer2 in *S. macrospora* depend on the interaction of Mer2 with the Mre11 complex.

CONCLUSIONS

Meiotic recombination, initiated by the induction of a large number of DNA DSBs, is an ancestral attribute of sexual reproduction. Comparison of the proteins required for meiotic DSB formation in distantly related organisms revealed a common phylogenetic origin. Our work reveals striking specificities of the meiotic DSB machinery in *Arabidopsis* compared to other eukaryotes, highlighting the diversity of mechanisms that were selected during evolution towards the achievement of a common purpose.

SUPPLEMENTARY DATA

Supplementary Data are available at NAR Online.

ACKNOWLEDGEMENTS

We wish to thank Fabien Nogué (IJPB, Versailles) for his help in CRISPR-Cas9 mutagenesis, Raphaël Mercier (MPIPZ, Cologne), Eric Jenczewski (IJPB, Versailles) and Marie-Therese Kurzbauer (Max Perutz Labs, Vienna) for critical discussions on the manuscript. We also wish to thank Chris West (University of Leeds) for sharing NBS1 yeast two-hybrid clones. The authors also thank Khalissa Bouchenine (IJPB, Versailles) for her help in Y2H and Lena Hess (Max Perutz Labs, Vienna) for helping with protein preparation for antibody production and the Max Perutz Labs light microscopy facility for technical support. The authors thank 'LKG Scientific editing' for proofreading the

manuscript. This work has benefited from the support of IJPB's Plant Observatory technological platforms.

FUNDING

FWF Austrian Science Fund (P18036, I1468, F3408, I3685); Agence Nationale de la Recherche (ANR-ESSPOIR-17-CE12-0032); Saclay Plant Sciences-SPS (ANR-17-EUR-0007). Funding for open access charge: ANR (ESSPOIR-17-CE12-0032).
Conflict of interest statement. None declared.

REFERENCES

1. Wang,S., Zickler,D., Kleckner,N. and Zhang,L. (2015) Meiotic crossover patterns: obligatory crossover, interference and homeostasis in a single process. *Cell Cycle*, **14**, 305–314.
2. Hunter,N. (2015) Meiotic recombination: the essence of heredity. *Cold Spring Harb. Perspect. Biol.*, **7**, a016618.
3. Mercier,R., Mézard,C., Jenczewski,E., Macaisne,N. and Grelon,M. (2015) The molecular biology of meiosis in plants. *Annu. Rev. Plant Biol.*, **66**, 297–327.
4. Zelkowski,M., Olson,M.A., Wang,M. and Pawlowski,W.P. (2019) Diversity and determinants of meiotic recombination landscapes. *Trends Genet.*, **35**, 359–370.
5. de Massy,B. (2013) Initiation of meiotic recombination: how and where? Conservation and specificities among eukaryotes. *Annu. Rev. Genet.*, **47**, 563–599.
6. Keeney,S., Lange,J. and Mohibullah,N. (2014) Self-organization of meiotic recombination initiation: general principles and molecular pathways. *Annu. Rev. Genet.*, **48**, 187–214.
7. Lukaszewicz,A., Lange,J., Keeney,S. and Jasin,M. (2018) Control of meiotic double-strand-break formation by ATM: local and global views. *Cell Cycle*, **17**, 1155–1172.
8. Yadav,V.K. and Claeys Bouuaert,C. (2021) Mechanism and control of meiotic DNA double-strand break formation in *S. cerevisiae*. *Front. Cell Dev. Biol.*, **9**, 642737.
9. Kurzbauer,M., Janisiw,M.P., Paulin,L.F., Prusén Mota,I., Tomanov,K., Krsicka,O., Haeseler,A. Von, Schubert,V. and Schlögelhofer,P. (2021) ATM controls meiotic DNA double-strand break formation and recombination and affects synaptonemal complex organization in plants. *Plant Cell*, **33**, 1633–1656.
10. Dereli,I., Stanzione,M., Olmeda,F., Papanikos,F., Baumann,M., Demir,S., Carofiglio,F., Lange,J., de Massy,B., Baarends,W.M. *et al.* (2021) Four-pronged negative feedback of DSB machinery in meiotic DNA-break control in mice. *Nucleic Acids Res.*, **49**, 2609–2628.
11. Robert,T., Vrielynck,N., Mézard,C., de Massy,B. and Grelon,M. (2016) A new light on the meiotic DSB catalytic complex. *Semin. Cell Dev. Biol.*, **54**, 165–176.
12. Grelon,M., Vezon,D., Gendrot,G. and Pelletier,G. (2001) AtSPO11-1 is necessary for efficient meiotic recombination in plants. *EMBO J.*, **20**, 589–600.
13. Stacey,N.J., Kuromori,T., Azumi,Y., Roberts,G., Breuer,C., Wada,T., Maxwell,A., Roberts,K. and Sugimoto-Shirasu,K. (2006) Arabidopsis SPO11-2 functions with SPO11-1 in meiotic recombination. *Plant J.*, **48**, 206–216.
14. Hartung,F., Wurz-Wildersinn,R., Fuchs,J., Schubert,I., Suer,S. and Puchta,H. (2007) The catalytically active tyrosine residues of both SPO11-1 and SPO11-2 are required for meiotic double-strand break induction in Arabidopsis. *Plant Cell*, **19**, 3090–3099.
15. Vrielynck,N., Chambon,A., Vezon,D., Pereira,L., Chelysheva,L.A., De Muyt,A., Mézard,C., Mayer,C. and Grelon,M. (2016) A DNA topoisomerase VI-like complex initiates meiotic recombination. *Science*, **351**, 939–943.
16. Fayos,I., Meunier,A.C., Vernet,A., Sanz,S.N., Portefaix,M., Lartaud,M., Bastianelli,G., Périn,C., Nicolas,A. and Guiderdoni,E. (2020) Assessment of the roles of OsSPO11-2 and OsSPO11-4 in rice meiosis using CRISPR/Cas9 mutagenesis. *J. Exp. Bot.*, **71**, 7046–7058.
17. Ku,J.-C., Ronceret,A., Golubovskaya,I., Lee,D.H., Wang,C., Timofejeva,L., Kao,Y.-H., Gomez Angoa,A.K., Kremling,K., Williams-Carrier,R. *et al.* (2020) Dynamic localization of SPO11-1 and conformational changes of meiotic axial elements during recombination initiation of maize meiosis. *PLoS Genet.*, **16**, e1007881.
18. Da Ines,O., Michard,R., Fayos,I., Bastianelli,G., Nicolas,A., Guiderdoni,E., White,C. and Sourdille,P. (2020) Bread Wheat TaSPO11-1 exhibits evolutionary conserved function in meiotic recombination across distant plant species. *Plant J.*, **103**, 2052–2068.
19. Robert,T., Nore,A., Brun,C., Maffre,C., Crimi,B., Guichard,V., Bourbon,H.M. and de Massy,B. (2016) The TopoVIB-Like protein family is required for meiotic DNA double-strand break formation. *Science*, **351**, 943–949.
20. Claeys Bouuaert,C., Tischfield,S.E., Pu,S., Mimitou,E.P., Arias-Palomo,E., Berger,J.M. and Keeney,S. (2021) Structural and functional characterization of the Spo11 core complex. *Nat. Struct. Mol. Biol.*, **28**, 92–102.
21. Keeney,S., Giroux,C.N. and Kleckner,N. (1997) Meiosis-specific DNA double-strand breaks are catalyzed by Spo11, a member of a widely conserved protein family. *Cell*, **88**, 375–384.
22. Neale,M.J., Pan,J. and Keeney,S. (2005) Endonucleolytic processing of covalent protein-linked DNA double-strand breaks. *Nature*, **436**, 1053–1057.
23. McKee,A.H. and Kleckner,N. (1997) A general method for identifying recessive diploid-specific mutations in Saccharomyces cerevisiae, its application to the isolation of mutants blocked at intermediate stages of meiotic prophase and characterization of a new gene SAE2. *Genetics*, **146**, 797–816.
24. Prinz,S., Amon,A. and Klein,F. (1997) Isolation of COM1, a new gene required to complete meiotic double-strand break-induced recombination in Saccharomyces cerevisiae. *Genetics*, **146**, 781–795.
25. Uanschou,C., Siwiec,T., Pedrosa-Harand,A., Kerzendorfer,C., Sanchez-Moran,E., Novatchkova,M., Akimcheva,S., Woglar,A., Klein,F. and Schlögelhofer,P. (2007) A novel plant gene essential for meiosis is related to the human CtIP and the yeast COM1/SAE2 gene. *EMBO J.*, **26**, 5061–5070.
26. Schaeper,U., Subramanian,T., Lim,L., Boyd,J.M. and Chinnadurai,G. (1998) Interaction between a cellular protein that binds to the C-terminal region of adenovirus E1A (CtBP) and a novel cellular protein is disrupted by E1A through a conserved PLDLS motif. *J. Biol. Chem.*, **273**, 8549–8552.
27. Fusco,C., Reymond,A. and Zervos,A.S. (1998) Molecular cloning and characterization of a novel retinoblastoma-binding protein. *Genomics*, **51**, 351–358.
28. Lam,I. and Keeney,S. (2014) Mechanism and regulation of meiotic recombination initiation. *Cold Spring Harb. Perspect. Biol.*, **7**, a016634.
29. Kumar,R., Oliver,C., Brun,C., Juarez-Martinez,A.B., Tarabay,Y., Kadlec,J. and de Massy,B. (2018) Mouse REC114 is essential for meiotic DNA double-strand break formation and forms a complex with MEI4. *Life Sci. Allian.*, **1**, e201800259.
30. Kumar,R., Bourbon,H.M. and De Massy,B. (2010) Functional conservation of Mei4 for meiotic DNA double-strand break formation from yeasts to mice. *Genes Dev.*, **24**, 1266–1280.
31. Tessé,S., Bourbon,H.M., Debuchy,R., Budin,K., Dubois,E., Liangran,Z., Antoine,R., Piolot,T., Kleckner,N., Zickler,D. *et al.* (2017) Asy2/Mer2: an evolutionarily conserved mediator of meiotic recombination, pairing, and global chromosome compaction. *Genes Dev.*, **31**, 1880–1893.
32. Tessé,S., Storlazzi,A., Kleckner,N. and Gargano,S. Zickler, D. (2003) Localization and roles of Ski8p protein in Sordaria meiosis and delineation of three mechanistically distinct steps of meiotic homolog juxtaposition. *Proc. Natl. Acad. Sci. USA*, **100**, 12865–12870.
33. Arora,C., Kee,K., Maleki,S. and Keeney,S. (2004) Antiviral protein Ski8 is a direct partner of Spo11 in meiotic DNA break formation, independent of its cytoplasmic role in RNA metabolism. *Mol. Cell*, **13**, 549–559.
34. Evans,D.H., Li,Y.F., Fox,M.E. and Smith,G.R. (1997) A WD repeat protein, Rec14, essential for meiotic recombination in Schizosaccharomyces pombe. *Genetics*, **146**, 1253–1264.
35. Jolivet,S., Vezon,D., Froger,N. and Mercier,R. (2006) Non conservation of the meiotic function of the Ski8/Rec103 homolog in Arabidopsis. *Genes Cells*, **11**, 615–622.
36. Boekhout,M., Karasu,M.E., Wang,J., Acquaviva,L., Pratto,F., Brick,K., Eng,D.Y., Xu,J., Camerini-Otero,R.D., Patel,D.J. *et al.*

(2019) REC114 partner ANKRD31 controls number, timing, and location of meiotic DNA breaks. *Mol. Cell*, **74**, 1053–1068.
37. Papanikos,F., Clément,J.A.J., Testa,E., Ravindranathan,R., Grey,C., Dereli,I., Bondarieva,A., Valerio-Cabrera,S., Stanzione,M., Schleiffer,A. *et al.* (2019) Mouse ANKRD31 regulates spatiotemporal patterning of meiotic recombination initiation and ensures recombination between X and Y sex chromosomes. *Mol. Cell*, **74**, 1069–1085.
38. Zhang,C., Song,Y., Cheng,Z.-H., Wang,Y.-X., Zhu,J., Ma,H., Xu,L. and Yang,Z.-N. (2012) The Arabidopsis thaliana DSB formation (AtDFO) gene is required for meiotic double-strand break formation. *Plant J.*, **72**, 271–281.
39. Zickler,D. and Kleckner,N. (1999) Meiotic chromosomes: integrating structure and function. *Annu. Rev. Genet.*, **33**, 603–754.
40. Blat,Y., Protacio,R.U., Hunter,N. and Kleckner,N. (2002) Physical and functional interactions among basic chromosome organizational features govern early steps of meiotic chiasma formation. *Cell*, **111**, 791–802.
41. Panizza,S., Mendoza,M.a., Berlinger,M., Huang,L., Nicolas,A., Shirahige,K. and Klein,F. (2011) Spo11-accessory proteins link double-strand break sites to the chromosome axis in early meiotic recombination. *Cell*, **146**, 372–383.
42. Sommermeyer,V., Béneut,C., Chaplais,E., Serrentino,M.E. and Borde,V. (2013) Spp1, a member of the Set1 Complex, promotes meiotic DSB formation in promoters by tethering histone H3K4 methylation sites to chromosome axes. *Mol. Cell*, **49**, 43–54.
43. Acquaviva,L., Székvölgyi,L., Dichtl,B., Dichtl,B.S., de La Roche Saint André,C., Nicolas,A. and Géli,V. (2013) The COMPASS subunit Spp1 links histone methylation to initiation of meiotic recombination. *Science*, **339**, 215–218.
44. Borde,V. and de Massy,B. (2013) Programmed induction of DNA double strand breaks during meiosis: setting up communication between DNA and the chromosome structure. *Curr. Opin. Genet. Dev.*, **23**, 147–155.
45. De Muyt,A., Pereira,L., Vezon,D., Chelysheva,L.A., Gendrot,G., Chambon,A., Lainé-Choinard,S., Pelletier,G., Mercier,R., Nogué,F. *et al.* (2009) A high throughput genetic screen identifies new early meiotic recombination functions in Arabidopsis thaliana. *PLoS Genet.*, **5**, e1000654.
46. Mercier,R. and Grelon,M. (2008) Meiosis in plants: ten years of gene discovery. *Cytogenet. Genome Res.*, **120**, 281–290.
47. Rossignol,P., Collier,S., Bush,M., Shaw,P. and Doonan,J.H. (2007) Arabidopsis POT1A interacts with TERT-V(I8), an N-terminal splicing variant of telomerase. *J. Cell Sci.*, **120**, 3678–3687.
48. Stellberger,T., Häuser,R., Baiker,A., Pothineni,V.R., Haas,J. and Uetz,P. (2010) Improving the yeast two-hybrid system with permutated fusions proteins: the Varicella Zoster Virus interactome. *Proteome Sci.*, **8**, 8.
49. Azimzadeh,J., Nacry,P., Christodoulidou,A., Drevensek,S., Camilleri,C., Amiour,N., Parcy,F., Pastuglia,M. and Bouchez,D. (2008) Arabidopsis TONNEAU1 proteins are essential for preprophase band formation and interact with centrin. *Plant Cell*, **20**, 2146–2159.
50. Chambon,A., West,A., Vezon,D., Horlow,C., De Muyt,A., Chelysheva,L., Ronceret,A., Darbyshire,A., Osman,K., Heckmann,S. *et al.* (2018) Identification of ASYNAPTIC4, a component of the meiotic chromosome axis. *Plant Physiol.*, **178**, 233–246.
51. De Muyt,A., Vezon,D., Gendrot,G., Gallois,J.-L., Stevens,R. and Grelon,M. (2007) AtPRD1 is required for meiotic double strand break formation in Arabidopsis thaliana. *EMBO J.*, **26**, 4126–4137.
52. Waterworth,W.M., Altun,C., Armstrong,S.J., Roberts,N., Dean,P.J., Young,K., Weil,C.F., Bray,C.M. and West,C.E. (2007) NBS1 is involved in DNA repair and plays a synergistic role with ATM in mediating meiotic homologous recombination in plants. *Plant J.*, **52**, 41–52.
53. Haeussler,M., Schönig,K., Eckert,H., Eschstruth,A., Mianné,J., Renaud,J.-B., Schneider-Maunoury,S., Shkumatava,A., Teboul,L., Kent,J. *et al.* (2016) Evaluation of off-target and on-target scoring algorithms and integration into the guide RNA selection tool CRISPOR. *Genome Biol.*, **17**, 148.
54. Ross,K.J., Fransz,P. and Jones,G.H. (1996) A light microscopic atlas of meiosis in Arabidopsis thaliana. *Chromosome Res.*, **4**, 507–516.
55. Armstrong,S.J. and Osman,K. (2013) Immunolocalization of meiotic proteins in Arabidopsis thaliana: method 2. *Methods Mol. Biol.*, **990**, 103–107.
56. Chelysheva,L.A., Grandont,L., Vrielynck,N., le Guin,S., Mercier,R. and Grelon,M. (2010) An easy protocol for studying chromatin and recombination protein dynamics during Arabidopsis thaliana meiosis: immunodetection of cohesins, histones and MLH1. *Cytogenet. Genome Res.*, **129**, 143–153.
57. Hurel,A., Phillips,D., Vrielynck,N., Mézard,C., Grelon,M. and Christophorou,N. (2018) A cytological approach to studying meiotic recombination and chromosome dynamics in Arabidopsis thaliana male meiocytes in three dimensions. *Plant J.*, **95**, 385–396.
58. Sims,J., Copenhaver,G.P. and Schlögelhofer,P. (2019) Meiotic DNA repair in the nucleolus employs a nonhomologous end-joining mechanism. *Plant Cell*, **31**, 2259–2275.
59. Chelysheva,L.A., Gendrot,G., Vezon,D., Doutriaux,M.-P., Mercier,R. and Grelon,M. (2007) Zip4/Spo22 is required for class I CO formation but not for synapsis completion in Arabidopsis thaliana. *PLoS Genet.*, **3**, e83.
60. Higgins,J.D., Sanchez-Moran,E., Armstrong,S.J., Jones,G.H. and Franklin,F.C.H. (2005) The Arabidopsis synaptonemal complex protein ZYP1 is required for chromosome synapsis and normal fidelity of crossing over. *Genes Dev.*, **19**, 2488–2500.
61. Cromer,L., Jolivet,S., Horlow,C., Chelysheva,L.A., Heyman,J., De Jaeger,G., Koncz,C., De Veylder,L. and Mercier,R. (2013) Centromeric cohesion is protected twice at meiosis, by SHUGOSHINs at anaphase I and by PATRONUS at interkinesis. *Curr. Biol.*, **23**, 2090–2099.
62. Kurzbauer,M.-T., Uanschou,C., Chen,D. and Schlögelhofer,P. (2012) The recombinases DMC1 and RAD51 are functionally and spatially separated during meiosis in Arabidopsis. *Plant Cell*, **24**, 2058–2070.
63. Chelysheva,L.A., Diallo,S., Vezon,D., Gendrot,G., Vrielynck,N., Belcram,K., Rocques,N., Márquez-Lema,A., Bhatt,A.M., Horlow,C. *et al.* (2005) AtREC8 and AtSCC3 are essential to the monopolar orientation of the kinetochores during meiosis. *J. Cell Sci.*, **118**, 4621–4632.
64. Ferdous,M., Higgins,J.D., Osman,K., Lambing,C., Roitinger,E., Mechtler,K., Armstrong,S.J., Perry,R., Pradillo,M., Cuñado,N. *et al.* (2012) Inter-homolog crossing-over and synapsis in Arabidopsis meiosis are dependent on the chromosome axis protein AtASY3. *PLos Genet.*, **8**, e1002507.
65. Chelysheva,L.A., Vezon,D., Chambon,A., Gendrot,G., Pereira,L., Lemhemdi,A., Vrielynck,N., Le Guin,S., Novatchkova,M. and Grelon,M. (2012) The Arabidopsis HEI10 is a new ZMM protein related to Zip3. *PLoS Genet.*, **8**, e1002799.
66. Fernandes,J.B., Duhamel,M., Seguéla-Arnaud,M., Froger,N., Girard,C., Choinard,S., Solier,V., De Winne,N., De Jaeger,G., Gevaert,K. *et al.* (2018) FIGL1 and its novel partner FLIP form a conserved complex that regulates homologous recombination. *PLoS Genet.*, **14**, e1007317.
67. Sims,J., Schlögelhofer,P. and Kurzbauer,M.-T. (2021) From microscopy to nanoscopy: defining an Arabidopsis thaliana meiotic atlas at the nanometer scale. *Front. Plant Sci.*, **12**, 672914.
68. Ronceret,A., Doutriaux,M.-P., Golubovskaya,I.N. and Pawlowski,W.P. (2009) PHS1 regulates meiotic recombination and homologous chromosome pairing by controlling the transport of RAD50 to the nucleus. *Proc. Natl. Acad. Sci. USA*, **106**, 20121–20126.
69. Tang,Y., Yin,Z., Zeng,Y., Zhang,Q., Chen,L., He,Y., Lu,P., Ye,D. and Zhang,X. (2017) MTOPVIB interacts with AtPRD1 and plays important roles in formation of meiotic DNA double-strand breaks in Arabidopsis. *Sci. Rep.*, **7**, 10007.
70. Yang,C., Sofroni,K., Wijnker,E., Hamamura,Y., Carstens,L., Harashima,H., Stolze,S.C., Vezon,D., Chelysheva,L., Orban-Nemeth,Z. *et al.* (2020) The Arabidopsis Cdk1/Cdk2 homolog CDKA;1 controls chromosome axis assembly during plant meiosis. *EMBO J.*, **39**, e101625.
71. West,A.M., Rosenberg,S.C., Ur,S.N., Lehmer,M.K., Ye,Q., Hagemann,G., Caballero,I., Usón,I., MacQueen,A.J., Herzog,F. *et al.* (2019) A conserved filamentous assembly underlies the structure of the meiotic chromosome axis. *Elife*, **8**, e40372.
72. Choi,K., Zhao,X., Tock,A.J., Lambing,C., Underwood,C.J., Hardcastle,T.J., Serra,H., Kim,J., Cho,H.S., Kim,J. *et al.* (2018) Nucleosomes and DNA methylation shape meiotic DSB frequency in

Arabidopsis thaliana transposons and gene regulatory regions. *Genome Res.*, **28**, 532–546.
73. Puizina,J., Siroky,J., Mokros,P., Schweizer,D. and Riha,K. (2004) Mre11 deficiency in Arabidopsis is associated with chromosomal instability in somatic cells and Spo11-dependent genome fragmentation during meiosis. *Plant Cell*, **16**, 1968–1978.
74. Robert,T., Nore,A., Maffre,C., Crimi,B., Brun,C., Bourbon,H.M. and de Massy,B. (2016) The TopoVIB-Like protein family is required for meiotic DNA double strand break formation. *Science (80-.).*, **351**, 943–949.
75. Libby,B.J., Reinholdt,L.G. and Schimenti,J.C. (2003) Positional cloning and characterization of Mei1, a vertebrate-specific gene required for normal meiotic chromosome synapsis in mice. *Proc. Natl. Acad. Sci. USA*, **100**, 15706–15711.
76. Reinholdt,L.G. and Schimenti,J.C. (2005) Mei1 is epistatic to Dmc1 during mouse meiosis. *Chromosoma*, **114**, 127–134.
77. Acquaviva,L., Boekhout,M., Karasu,M.E., Brick,K., Pratto,F., Li,T., van Overbeek,M., Kauppi,L., Camerini-Otero,R.D., Jasin,M. *et al.* (2020) Ensuring meiotic DNA break formation in the mouse pseudoautosomal region. *Nature*, **582**, 426–431.
78. Henderson,K.a, Kee,K., Maleki,S., Santini,P.a and Keeney,S. (2006) Cyclin-dependent kinase directly regulates initiation of meiotic recombination. *Cell*, **125**, 1321–1332.
79. Kariyazono,R., Oda,A., Yamada,T. and Ohta,K. (2019) Conserved HORMA domain-containing protein Hop1 stabilizes interaction between proteins of meiotic DNA break hotspots and chromosome axis. *Nucleic Acids Res.*, **47**, 10166–10180.
80. Miyoshi,T., Ito,M., Kugou,K., Yamada,S., Furuichi,M., Oda,A., Yamada,T., Hirota,K., Masai,H. and Ohta,K. (2012) A central coupler for recombination initiation linking chromosome architecture to S phase checkpoint. *Mol. Cell*, **47**, 722–733.
81. Stanzione,M., Baumann,M., Papanikos,F., Dereli,I., Lange,J., Ramlal,A., Tränkner,D., Shibuya,H., de Massy,B., Watanabe,Y. *et al.* (2016) Meiotic DNA break formation requires the unsynapsed chromosome axis-binding protein IHO1 (CCDC36) in mice. *Nat. Cell Biol.*, **18**, 1208–1220.
82. Li,J., Hooker,G.W. and Roeder,G.S. (2006) Saccharomyces cerevisiae Mer2, Mei4 and Rec114 form a complex required for meiotic double-strand break formation. *Genetics*, **173**, 1969–1981.
83. Sanchez-Moran,E., Santos,J.-L., Jones,G.H. and Franklin,F.C.H. (2007) ASY1 mediates AtDMC1-dependent interhomolog recombination during meiosis in Arabidopsis. *Genes Dev.*, **21**, 2220–2233.
84. Maleki,S., Neale,M.J., Arora,C., Henderson,K.a and Keeney,S. (2007) Interactions between Mei4, Rec114, and other proteins required for meiotic DNA double-strand break formation in Saccharomyces cerevisiae. *Chromosoma*, **116**, 471–486.
85. Walker,J., Gao,H., Zhang,J., Aldridge,B., Vickers,M., Higgins,J.D. and Feng,X. (2018) Sexual-lineage-specific DNA methylation regulates meiosis in Arabidopsis. *Nat. Genet.*, **50**, 130–137.
86. Bellani,M.a, Boateng,K.a, McLeod,D. and Camerini-Otero,R.D. (2010) The expression profile of the major mouse SPO11 isoforms indicates that SPO11beta introduces double strand breaks and suggests that SPO11alpha has an additional role in prophase in both spermatocytes and oocytes. *Mol. Cell. Biol.*, **30**, 4391–4403.
87. Stamper,E.L., Rodenbusch,S.E., Rosu,S., Ahringer,J., Villeneuve,A.M. and Dernburg,A.F. (2013) Identification of DSB-1, a protein required for initiation of meiotic recombination in Caenorhabditis elegans, illuminates a crossover assurance checkpoint. *PLoS Genet.*, **9**, e1003679.
88. Rosu,S., Zawadzki,K.a., Stamper,E.L., Libuda,D.E., Reese,A.L., Dernburg,A.F. and Villeneuve,A.M. (2013) The C. elegans DSB-2 protein reveals a regulatory network that controls competence for meiotic DSB formation and promotes crossover assurance. *PLoS Genet.*, **9**, e1003674.
89. Malone,R.E., Bullard,S., Hermiston,M., Rieger,R., Cool,M. and Galbraith,a. (1991) Isolation of mutants defective in early steps of meiotic recombination in the yeast Saccharomyces cerevisiae. *Genetics*, **128**, 79–88.
90. Pittman,D., Lu,W. and Malone,R.E. (1993) Genetic and molecular analysis of REC114, an early meiotic recombination gene in yeast. *Curr. Genet.*, **23**, 295–304.
91. Molnar,M., Parisi,S., Kakihara,Y., Nojima,H., Yamamoto,A., Hiraoka,Y., Bozsik,A., Sipiczki,M. and Kohli,J. (2001) Characterization of rec7, an early meiotic recombination gene in Schizosaccharomyces pombe. *Genetics*, **157**, 519–532.
92. Pawlowski,W.P., Golubovskaya,I.N., Timofejeva,L., Meeley,R.B., Sheridan,W.F. and Cande,W.Z. (2004) Coordination of meiotic recombination, pairing, and synapsis by PHS1. *Science*, **303**, 89–92.
93. Ji,J., Tang,D., Shen,Y., Xue,Z., Wang,H., Shi,W., Zhang,C., Du,G., Li,Y. and Cheng,Z. (2016) P31comet, a member of the synaptonemal complex, participates in meiotic DSB formation in rice. *Proc. Natl. Acad. Sci. USA*, **113**, 10577–10582.
94. Miao,C., Tang,D., Zhang,H., Wang,M., Li,Y., Tang,S., Yu,H., Gu,M. and Cheng,Z. (2013) Central region component1, a novel synaptonemal complex component, is essential for meiotic recombination initiation in rice. *Plant Cell*, **25**, 2998–3009.
95. Balboni,M., Yang,C., Komaki,S., Brun,J. and Schnittger,A. (2020) COMET functions as a PCH2 cofactor in regulating the HORMA domain protein ASY1. *Curr. Biol.*, **30**, 4113–4127.
96. Yang,C., Hu,B., Portheine,S.M., Chuenban,P. and Schnittger,A. (2020) State changes of the HORMA protein ASY1 are mediated by an interplay between its closure motif and PCH2. *Nucleic Acids Res.*, **48**, 11521–11535.
97. Lambing,C., Osman,K., Nuntasoontorn,K., West,A., Higgins,J.D., Copenhaver,G.P., Yang,J., Armstrong,S.J., Mechtler,K., Roitinger,E. *et al.* (2015) Arabidopsis PCH2 mediates meiotic chromosome remodeling and maturation of crossovers. *PLoS Genet.*, **11**, e1005372.
98. Chaw,S.-M., Chang,C.-C., Chen,H.-L. and Li,W.-H. (2004) Dating the monocot-dicot divergence and the origin of core eudicots using whole chloroplast genomes. *J. Mol. Evol.*, **58**, 424–441.
99. Claeys Bouuaert,C., Pu,S., Wang,J., Oger,C., Daccache,D., Xie,W., Patel,D.J. and Keeney,S. (2021) DNA-driven condensation assembles the meiotic DNA break machinery. *Nature*, **592**, 144–149.